Performance Analysis Of Multilevel Heliostat Field Layout

Ra'ad K Mohammed Aldulaimi[1,2*] and Mehmet Sait Söylemez[1]
[1]Department of Mechanical Engineering, University of Gaziantep, 27310 Gaziantep, Turkey
[2] University of Baghdad, Baghdad, Iraq
*rd13434@mail2.gantep.edu.tr

Abstract

A novel heliostat field layout is suggested by dividing specified heliostats located farthest from the tower and exhibiting low optical efficiency into strips and increasing the height for these strips with varying heights, based on the consideration of no blocking. A novel geometrical equation is presented for this purpose, and the results indicate an increase in the total annual efficiency of the field. The proposed layout is implemented on an optimized heliostat field consisting of 2650 SENER heliostats, based on the data obtained using Gemasolar in Seville, Spain, which is used as a reference in this work. Each heliostat position is specified using an optimization algorithm that refines previously proposed models, and two parameters are added to this model to further optimize the heliostat layout.

Keywords: Solar Power Tower Plant, Multilevel Layout, Simulation, Heliostat Field.

Değişken Seviyeli Heliostat Uygulamalı Güneş Tarlalarının Performans Değerlendirmesi

Özet

Güneş tarlalarında optik verimliliği temelde helyostatlardaki gölgelemeleri engelleyerek arttırmak amacıyla, kademeli değişken yükseklik uygulamasının etkisi araştırılmış ve düşük optik verimlilik değerlerinin düzeldiği görülmüştür. Bu amaçla, geliştirilen bir geometrik denklem sunulmuş ve sonuçlarda güneş tarlasında yıllık verimin arttığı hesaplanmıştır. Önceden optimize edilmiş 2650 helyostatlı SENER güneş tarlası için önerilen yöntem kullanılarak, İspanyanın Sevilla şehrinde bulunan Gemasolar helyostat sistemi için alınan sonuçlar önceki değerlerle karşılaştırılmak suretiyle mukayeseli olarak kontrol edilerek doğrulanmıştır. Her bir helyostat pozisyonu için optimizasyon algoritması tanımlanarak önceki modellemelerin önüne geçen ve iki yeni parametreyi de ekleyerek helyostat yerleştirilmesini optimize eden bir yeni model önerilmiştir.

Anahtar Kelimeler: Güneş Enerjili Güç Üretimi, Değişken Seviyeli Helyostat Yerleşimi, Modelleme, Heliostat Tarlası

1. Introduction

Solar power tower plants (SPTPs) offer a unique method for achieving highly focused solar radiation on a large scale for electrical power generation, among other applications [1]. SPTPs use several hundred or even thousands of reflectors, called heliostats, as intermediate optical devices between the sun's rays and the energy absorbing device. The heliostats are set around a receiver that follows the sun, and the reflection of the light further focuses it up to 1000 times to a central receiver placed at the central point on the top of a high tower. A computer controls each heliostat's rotation around two axes to ensure continually correct directing, with a tracking error of less than a fraction of a degree.

The ideal layout of the heliostat field is of primary importance and the topic of many studies, mainly because the heliostat approach accounts for 50% of the full price of the scheme, and the annual energy loss is approximately 47% [2]. Several codes have been produced for this purpose dating from the 1970s, and most of those codes are presented in [3]. For the most part, the most recent codes [4–7] identify various forms of access to increase the global optical efficiency (η).

On the other hand, because any SPTP optimization operation should depend on the annual energy estimation of each different layout, the insolation-weighted mean yearly

heliostat field efficiency $(\eta_{year,Eb})$ was calculated in [4], using Eq. (1):

$$\eta_{year,Eb} = \frac{\sum_{day=1}^{365} \int_{sunrise}^{sunset} E_b(t)\eta(t)dt}{\sum_{day=1}^{365} \int_{sunrise}^{sunset} E_b(t)dt} \qquad (1)$$

and for a compromise between CPU time and resolution, specify the 21st of each month during the year (average day), and carry out over all days the same function with all computations that are related to the other parameters of optical efficiency [6].

The annual energy is the integrated sum of the instantaneous energy transformed by all heliostats over time [8]. The positioning of the heliostats around the tower is a critical factor because the amount of energy collected at the receiver, for a given position of the sun, is a function of the position and form of the heliostats. Therefore, several papers have suggested changing the level of heliostat positions.

For instance, in [1], the authors derived a graphical method to plan a radially staggered solar field layout, limited by the consideration that no blocking losses would be sustained over the year. This method distributed heliostats in the field by specifying the placement of each one along an inclined plane, assuring that neighboring mirrors block none of the energy reflected by any given heliostat. Further limiting this study, the inclination of the ground of heliostat field was considered to cover the entire field area. This results in an inefficient and expensive process because the efficiency factor balance may be negatively affected, for instance, with shadow losses. Nonetheless, this method is suitable for preliminary heliostat field designs.

In [9], a Fortran computer program is the implemented to investigate square, circular, or mixed heliostats in the solar field layout. This discretization method computed shadowing and blocking losses, and compared the optical performances of different solar fields, including comparisons between flat and inclined grounds, assuming an inclined ground with a slope of $15°$ in the northern quadrant. This study showed that the inclined ground inhibits the increase of shadow losses with respect to the ground.

Most studies are based on an inclined ground with a fixed slope for all heliostats, and therefore low-level heliostats could be shaded by higher-level heliostats. Therefore, this study first develops the model presented in [1] and implements the layout presented in [4], which was shown to have greater overall efficiency by considerably reducing the requisite land area relative to the radially staggered layout. Second, this study investigates changing heliostat levels with no blocking consideration, but with variable slope, starting with the heliostat located farthest from the tower's central receiver because it has higher optical losses than the closer heliostats.

2. Simulation Tools

2.1. Instantaneous optical efficiency factors

The factors of optical efficiency, which presented energy losses associated with the heliostat field, given by Eq. (2):

$$\eta = \eta_{ref} \times \eta_{cos} \times \eta_{at} \times \eta_{in} \times \eta_{s\&b} \qquad (2)$$

in which η_{ref} represents the reflectivity of the heliostats, and η_{cos} represents the cosine of the incidence angle between the sun rays and the heliostat normal (θ), η_{at} Represents the atmospheric attenuation efficiency, which accounts for radiation losses in the distance (D) between a heliostat and the receiver, which can be estimated by Eqs. (3) and (4) as presented in [4,5]:

$$\eta_{at} = 0.99321 - 0.000176D + 1.97 \times 10^{-8}D^2 \qquad D \leq 1000m \qquad (3)$$
$$\eta_{at} = e^{-0.0001106D} \qquad D > 1000m \qquad (4)$$

η_{in} represents the interception efficiency, which related to Energy directed to the receiver that does not fall on the absorbing area, because of, the reflector surface accuracy, beam spread, mirror canting accuracy, and tracking accuracy all have a major effect on the flux distribution at the receiver, etc. An analytical flux density model or The HFLCAL model presented in [5,10,11], that simple and accurate tools applied to estimate the (η_{in}) in this study.The HFLCAL model integrated the flux distribution along an absorbing surface of the receiver to get the

intercepted power at a certain point in time, given by Eq. (5)

$$\eta_{in} = \frac{1}{2\pi\sigma_{tot}^2} \int_{(r_x)} \int_{(r_y)} e^{\left(-\frac{r_x^2 + r_y^2}{2\sigma_{tot}^2}\right)} dr_y \, dr_x \quad (5)$$

The coordinates r_x and r_y related to the vertical plane of the receiver, and (σ_{tot}) is the total dispersion of the flux distribution and is expressed by Eq. (6)

$$\sigma_{tot} = \frac{\sqrt{D^2\left(\sigma_{sun}^2 + \sigma_{bq}^2 + \sigma_{ast}^2 + \sigma_t^2\right)}}{\sqrt{\cos rec}} \quad (6)$$

Where, $\left(\sigma_{sun}, \sigma_{bq}, \sigma_{ast}, \sigma_t\right)$ namely sun shape error, Beam quality, the astigmatic effect, the tracking error, respectivly, and $(\cos rec)$ is the incidence cosine of the reflected central ray from the heliostat on the receiver surface (a vertical plane).Further details about HFLCAL functions and constants value can be found in Refs.[5].

$\eta_{s\&b}$ represents the shading and blocking efficiency. Shading often takes place when a heliostat shaded from the sunlight by an adjoining heliostat or a tower, and similarly blocking occurs if a heliostat block the sun rays reflected from an adjoining to the receiver, In this paper, the central ray tracing and discretization technique, which presented in [4], was adapted to calculate the $(\boldsymbol{\eta_{s\&b}})$ with small subdivisions and high accuracy.

2.2 Solar radiation

The annual energy from the receiver is the sum of the instantaneous energies produced by the heliostat field. After transforming the solar radiation along time increments sampled from the American Society of Heating, Refrigeration, and Air-conditioning Engineers (ASHRAE) Clear-sky Radiation Model [12], and utilizing two monthly factors and the relative air mass(m), which can be estimated by Eq. (7):

$$m = \frac{1}{\sin\alpha + 0.50572(6.07995 + \alpha)^{-1,6364}} \quad (7)$$

Where (α) represents the solar altitude angle and is expressed in degrees. The beam normal radiation E_b is given by Eq. (8):

$$E_b = E_o exp[-\tau_b m^b] \quad (w/m^2) \quad (8)$$

in which the beam's air mass exponents b are given by Eq. (9):

$$b = 1.219 - 0.043\tau_b - 0.151\tau_d - 0.204\tau_b\tau_d \quad (9)$$

and E_o is the extraterrestrial normal irradiance accumulated following Eq. (10):

$$E_o = E_{sc}\left(1 + 0.033cos\left(360^o \frac{(n_d - 3)}{365}\right)\right)$$

$$(w/m^2) \quad (10)$$

In Eq. (10), E_{sc} is equal to 1366.1 W/m², n_d is the day number, and τ_b and τ_d represent the apparent beam and diffusion optical depths, which are site specific and change during the year. For Seville, Spain, and other cities that study SPTP technology, these last parameters are given in [12] for each city on the 21st day of each month.

2.3 Heliostat and receiver specifications

Gemasolar, an SPTP in Seville, Spain, is the plant used as a reference in this work. The complete dimensions of the SENER heliostats utilized in Gemasolar are presented in [5, 13, 14]; the field parameters used in this study are presented in Table 1.

Table 1. Gemasolar field and receiver parameters [5,13,14]

Heliostats		Effective reflectivity, η_{ref}	0.88×0.95
Width W_h (m)	12.305	Heliostat numbers	2650
Height H_h (m)	9.752	**Receiver**	
Heliostat total diagonal, d_h (m)	15.7	Tower optical height h_t (m)	140
Heliostat total area, A_h (m²)	120	Receiver radius R_r (m)	4
Heliostat mirror area, A_m (m²)	115.7	Receiver height H_r (m)	9

2.4 Coordinate system

In the selection coordinate system (referred to in the following text as "tower system of coordinates"), east is in the positive

(y) direction, and north is in the positive (z) direction, while the zenith is in the (x) direction, as Fig (1) shows.
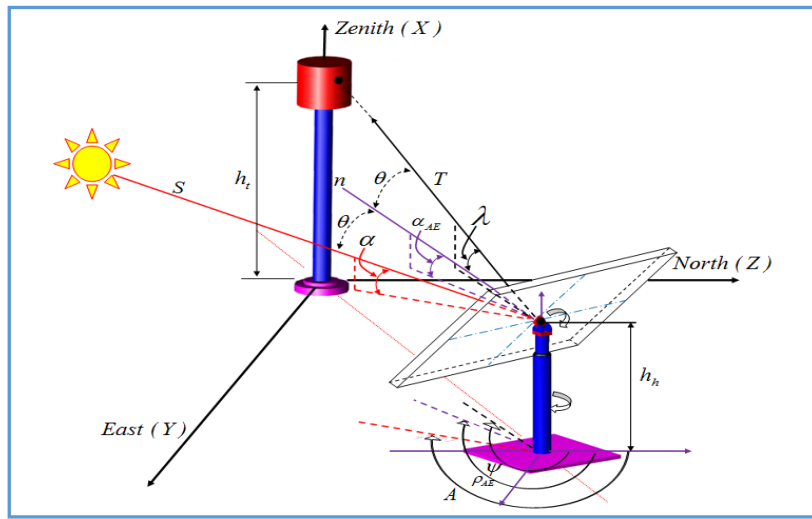
Figure 1. System Coordinate for heliostat fields and receiver

Given that the sun is a moving object while the receiver is a fixed object, the normal (n) of the heliostat has to adjust when the sun position changes with time, to ensure that the heliostat is oriented at the necessary angles.

The incident angle on the heliostat (θ) Similar to the angle of reflection, as indicated by Snell's law of reflection, then, the bisector of (s) and (T) is the heliostat normal (n), as shown in Eq. (11):

$$n = \frac{s + T}{|s + T|} \qquad (11)$$

The unit vector (s) refers to the sun and is estimated as presented in Ref. [15] depending upon Solar altitude angle(α) and Solar azimuth angle(A). The unit vector (T) is directed toward the aim point (receiver). Thus, vector (T) is in the direction of the central reflected ray.

To determine the (η) of the heliostat, the heliostat position frame should be estimated. The altered orientation of the frame during the sun tracking period in three-dimensional space can modeled by applying the coordinate transformation, which presented in Ref. [16]. The rest position or the initial coordinate of the frame is first defined in a fixed coordinate system. When the plane of the heliostat is parallel to the x-y plane, and the normal to its surface(n) is directed to the north direction,

The reflector is oriented using an actuator for rotation in the coordinate transformation for the Azimuth-Elevation *(AE)* sun-tracking method as presented in Ref. [17]. The first rotation transformation by the angle (α_{AE}) about the Y-axis will transform the point from the fixed coordinate system to an elevation-movement coordinate system. The second rotation transformation for the rotational

movement by the angle (ρ_{AE}) about the X-axis will transform the point of the elevation-movement coordinate system to the azimuth-movement coordinate system.

3. Mathematical Model for Multilevel Heliostat Field Layout

The positioning of the heliostats around the tower is an essential step that depends on many factors. On the other hand, the annual optical efficiency is considered to be the main factor for evaluating different field layouts. The procedure for estimating new heliostat elevations in a field layout with gradually varying successive heliostat levels is summarized in the following steps.

First, the layout of the heliostat field and the position for each heliostat, is defined based on the model presented in [4], which was inspired by the spiral patterns of the phyllotaxis disc. This layout was shown to increase overall efficiency and is expressed by Eqs. (12) and (13) as presented in [4] :

$$\theta_p = 2\pi\varphi^{-2}n_h \qquad (12)$$
$$r_{hp} = an_h^b \qquad (13)$$

Where θ_p represents the polar position angle for heliostats in the field, r_{hp} represents the radial position of the heliostat, and a and b represent field layout design variables. From Eqs. (12) and (13), evaluations of the different layouts are verified by forming various layout distributions with adjustments to the a and b parameters, using an optimization algorithm to estimate the best a and b values. The limits of a and b are assumed to be [2, 8] and [0.4, 0.7], respectively. A feature of the created heliostat field that is larger than the heliostat number for the necessary range uses Eqs. (12) and (13). Therefore, this study started with 5000 heliostats, with the objective of restricting the field to determine the optimal layout of 2650 heliostats.

The field size was selected to include 2650 heliostats, for comparison with the case study model. The distance between the heliostat and its neighbors is the main condition that must be specified before optimizing the field, to prevent overlap from occurring among the close circles

in which the heliostats move. Therefore, a program was written such that layouts that lead to interference between the circle movements for the heliostats were not considered. Furthermore, the diagonal of the total reflector area d_h equals 15.7 m for SENER heliostats (see Table 1) and the proposed code does not consider any extra separation distance ($d_{sep} = 0$).

In this study, a genetic algorithm (GA) is used to implement the necessary optimization duty because GA is one of the most efficient optimization methods. Successive random values of the design variables are inputted until the highest value of $\eta_{year,Eb}$ is recorded; in this case, the a and b parameters were 3.55 and 0.675, respectively, corresponding to a layout with 2650 heliostats.

These $\eta_{year,Eb}$ results based on the specified a and b parameters compare with other values of the same parameters for other studies [4] and [6] which used the same heliostat dimensions and layout, and the results show the higher performance than others with new values of parameters.

The second comparison is targeted by computing the value of the field efficiency in GEMASOLAR with modeling results of Ref. [5], depending on the same reference data, and considering the same model of solar radiation, where the values of solar radiation of the Ref. [5] started from $(15°)$ of sun elevations over horizontal. Even more than $(15°)$, some values range from $(17°)$, and end at noon, and shorthand all year by 35 steps at a time. The comparison shows that the result (57.3693%) are very close to the published data of Ref. [5], which equal (57.232%).

In the process of estimating the annual efficiency, several conditions become apparent: that the farthest heliostat from a tower has less optical efficiency, and heliostats closer to the tower and to the north exhibit higher cosine effect efficiency.

From these conditions, a new rear heliostat field arrangement is derived, arranging heliostats at different levels, such that no blocking losses occur throughout the year, with implementing the same layout model. To enhance the performance of these heliostats, the heliostats height is increased for selected heliostats located

15

at the edge of the field layout, which exhibit the lowest optical efficiency. This arrangement can be formulated mathematically from purely geometrical considerations.

The farthest heliostat in the layout, which experiences the highest blocking losses, is considered as a reference to delineate heliostat strips. In addition, the numbers and radii of successive heliostats are specified in relation to this reference heliostat farthest from the tower; successive heliostats are located in the same spiral line as the reference heliostat.

The successive heliostats are numbered for reference, considering the farthest heliostat as number one, and then heliostats that have a radius value between one and two are identified. This group represents the first strip. The same operation is conducted to identify subsequent strips.

The new height for all heliostats in the first strip is determined by representing the reference heliostat with its successive heliostat in a front view as shown in Fig. 2 by the circles (he_{c1}, he_{c2}). Subsequently, a straight tangential line (l_{ta}) is drawn from the point (T_p) on the lower edge of the receiver to the point tangent to the circle (he_{c2}), while increasing the circle's height (he_{c1}) with the same radius position until the circle becomes tangent to line (l_{ta}). In this configuration, (l_{ta}) represents the lowest limit of reflected rays originating behind the heliostat described by (he_{c2}) that also hit the receiver with no blocking by (he_{c1}).

The geometrical steps to derive Eq. (14) described below in Fig. 2 which is implemented to calculate the new height for all heliostats in the first strip, depending on the no blocking method illustrated in Fig. 2.
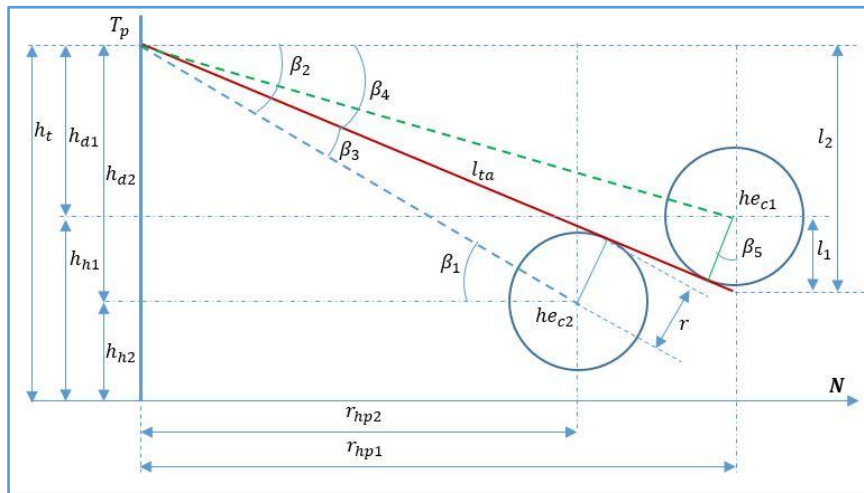
**Figure 2.** Front view of the reference and successive heliostats.

$$h_{h1} = h_t - \left(\left(\tan\left(\left(\tan^{-1}\frac{h_{d2}}{r_{hp2}} \right) - \left(\sin^{-1}\frac{r}{\sqrt{h_{d2}^2 + r_{hp2}^2}} \right) \right) \times r_{hp1} \right) - \left(\frac{r}{\cos\left(\left(\tan^{-1}\frac{h_{d2}}{r_{hp2}} \right) - \left(\sin^{-1}\frac{r}{\sqrt{h_{d2}^2 + r_{hp2}^2}} \right) \right)} \right) \right) \tag{14}$$

Where, $r = H_h/2$ and, $h_{d2} = h_t - h_{h(old)}$ The same procedure is used to determine the height for heliostats in the second strip by considering the two strips beyond the one under investigation, again with no blocking of the heliostats in the third strip, as shown in Fig. 3. With the new heights (h_{h1}, h_{h2}) for the first and second strips, from Eq. (14), while the height of the second strip is added to the difference in elevation of the first strip, as shown in Eq. (15):

$$h_{h1} = (h_{h1} - h_{h(old)}) + h_{h2} \tag{15}$$
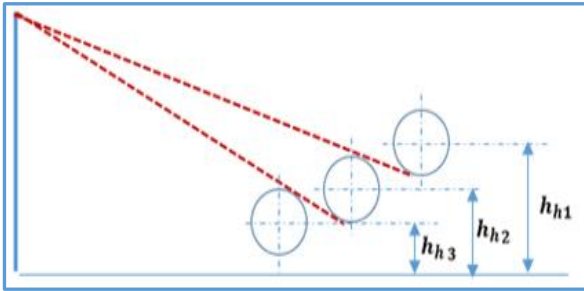
Figure 3. Increasing height of two successive strips.

Rising to three strips, Eq. (15) becomes Eqs. (16) and (17):

$$h_{h1} = (h_{h1} - h_{h(old)}) + (h_{h2} - h_{h(old)}) + h_{h3} \tag{16}$$

$$h_{h2} = (h_{h2} - h_{h(old)}) + h_{h3} \tag{17}$$

In this way, Eq. (14) is implemented three times, and the height of each strip is added to the difference in elevation for subsequent strips, as many times as necessary.

4. Analysis of increased height for certain groups of heliostats

As previously mentioned, the main objectives for this paper is to study the increased height of specified strips of heliostats that are located farthest from the tower and exhibit the highest optical losses in the heliostat field. The main objective of this analysis is to determine the optimal number of strips with increased height. Fig. 4 shows $\eta_{year,Eb}$ results for gradually and sequentially increasing the heights of different numbers of strips, where the first strip is farthest from the tower. Eight is shown to be the optimal number of strips in this heliostat field; after that, the value of $(\eta_{year,Eb})$ becomes approximately constant.
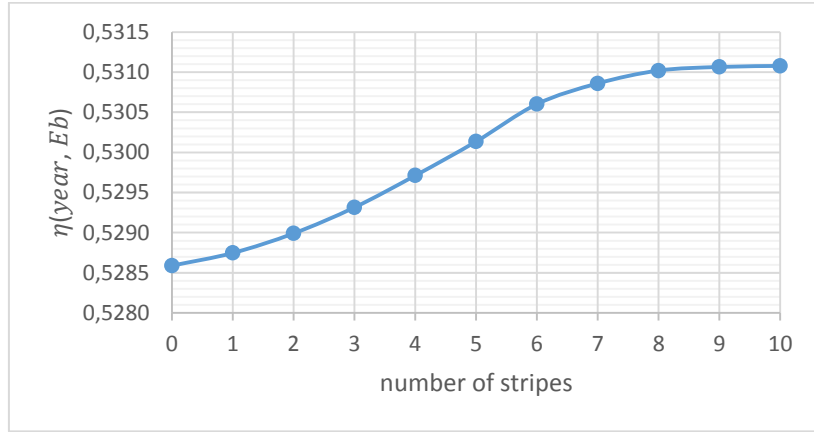
Figure 4. Mean yearly heliostat field efficiency $\eta_{year,Eb}$ with increasing the heights of different numbers of strips.

The reason for fixing $\eta_{year,Eb}$ is shown in Fig. 5, which illustrates that the heliostat strips are formed of different lengths. In addition, strips in the farthest regions become similar to straight line, and a few circumvent the line because of the small number of heliostats they contain. As a result, the shadow losses in successive strips are very small or nonexistent; as they get closer to the tower, the length of the strips begins to increase and assumes a horseshoe shape, as shown in Fig. 5. These horseshoe-shaped strips begin to rotate around the field, and shadow losses increase as the strips get closer to the tower, until plateauing at eight strips.
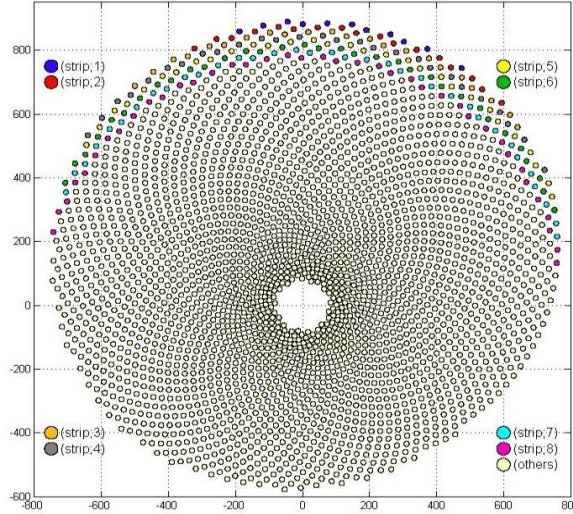
Figure 5. Eight heliostat strips encircling the center of the tower

After increasing the heights of the eight strips based on Eq. (14), we noted an increase in the blocking efficiency of the eight strips, offset by increased shadow losses for heliostats placed in front of the strips, as well as a slight decrease in η_{cos} appear with increasing numbers of strips.

As a result of the increased heights of the eight strips, $\eta_{year,Eb}$ increased from 52.86% to 53.10%, and the average increase in $\eta_{year,Eb}$ for each strip with increased height was in the range from 8.5% to 9.1%, as Table 2 shows. The overall efficiency of the proposed heliostat field is presented in Fig. 6.
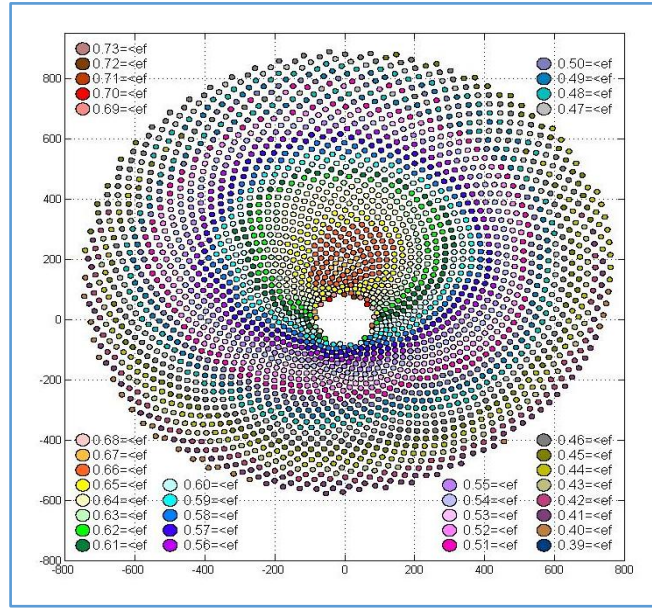
18

Figure 6. $\eta_{year,Eb}$ for the full heliostat field after increasing heights for eight strips

Table 2. Average increase in annual efficiency $\eta_{year,Eb}$ with increasing heights for successive strips

Number of strips	1	2	3	4	5	6	7	8
Height difference (m)[*]	60.49	52.74	45.07	37.41	29.80	22.26	14.78	7.35
Number of heliostats in each strip	11	17	22	27	30	33	35	39
Average net increase in $\eta_{year,Eb}$	9.1%	9%	8.91%	8.85%	8.8%	8.7%	8.6%	8.5%
[*] Height difference (m) = increased height – height without increasing								

5. Conclusion

A novel geometrical equation presented for the purpose of optimizing the heliostat field layout by increasing the height of specified heliostats exhibiting the lowest optical. Changes in heliostat levels with no blocking consideration are investigated, and heliostat located farthest from the tower's central receiver is considered. The results showed that the proposed layout increases the overall $\eta_{year,Eb}$ from 52.86% to 53.10%, and selected heliostat strips increased in the range between 8.5% and 9.1%.

6. Nomenclature

η	Instantaneous optical efficiency
η_{cos}	Cosine efficiency
η_{at}	Atmospheric attenuation efficiency
η_{in}	Interception efficiency
$\eta_{s\&b}$	Shading and blocking efficiency
η_{ref}	Reflectivity
$\eta_{year,Eb}$	Yearly insolation weighted efficiency
α	Solar altitude angle, rad
θ	Angle of incidence, rad
θ_P	polar position Angle for heliostat in the field
α_{AE}	Angular movements of the heliostat frame about the elevation axis
ρ_{AE}	Angular movements of the heliostat frame about the azimuth axis
λ	Orientation angle of heliostat
ψ	Angle position for heliostat
φ	Golden ratio $\left(1 + \sqrt{5}\right)/2 = 1.618$
A	Solar azimuth angle, rad
A_h	Heliostat total area
A_m	Heliostat mirror area
D	the distance between the heliostat Centre and the aim point in the receiver, m
d_h	Diagonal diameter of the total Heliostat
$E_b(t)$	Beam normal radiation, W/m²
E_o	Extraterrestrial normal irradiance, w/m^2
h_t	Tower optical height
n_d	Day number
n_h	Number of heliostat in the field
$\vec{n}$	The unit normal vector of the heliostat surface
r_{hP}	Radius position for heliostat

19

$\vec{s}$	The unit vector from the center of the heliostat pointing to the sun
$\vec{T}$	The unit vector from the center of the heliostat pointing to the tower
W_h, H_h	Width & Height of the heliostat
H_r, R_r	Height & radius of the Receiver height

7. References

1. F.M.F. Siala, M.E. Elayeb, Mathematical formulation of a graphical method for a no-blocking heliostat field layout, Renewable Energy 23 (2001) 77–92.

2. X. Wei, Z. Lu, W. Yu, Z. Wang, A new code for the design and analysis of the heliostat field layout for power tower system, Sol. Energy 84 (2010) 685–690.

3. P. Garcia, A. Ferriere, J.-J. Bezian, Codes for solar flux calculation dedicated to central receiver system applications: a comparative review, Sol. Energy 82 (2008) 189–197.

4. C.J. Noone, M. Torrilhon, A. Mitsos, Heliostat field optimization: a new computationally efficient model and biomimetic layout, Sol. Energy 86 (2012) 792–803.

5. F.J. Collado, J. Guallar, A review of optimized design layouts for solar power tower plants with campo code, Renewable Sustainable Energy Rev. 20 (2013) 142–154.

6. S.M. Besarati, D.Y. Goswami, A computationally efficient method for the design of the heliostat field for solar power tower plant, Renewable Energy 69 (2014) 226–232.

7. M. Chiesi, L. Vanzolini, E.F. Scarselli, R. Guerrieri, Accurate optical model for design and analysis of solar fields based on heterogeneous multicore systems, Renewable Energy 55 (2013) 241–251.

8. F.J. Collado, J. Guallar, Campo: generation of regular heliostat fields, Renewable Energy 46 (2012) 49–59.

9. E. Leonardi, B. D'Aguanno, CRS4-2: a numerical code for the calculation of the solar power collected in a central receiver system, Energy 36 (2011) 4828–4837.

10. M. Schmitz, P. Schwarzbozl, R. Buck, R. Pitz-Paal. Assessment of the potential improvement due to multiple apertures in central receiver systems with secondary concentrators. Solar Energy 80 (2006) 111–120.

11. F. J. Collado, One-point fitting of the flux density produced by a heliostat. Solar Energy 84 (2010) 673–684

12. American Society of Heating, Refrigerating, and Air-Conditioning Engineers (ASHRAE), 2013 ASHRAE Handbook - Fundamentals (SI); Climatic Design Information, ASHRAE, Georgia, USA, 2013.

13. J.I. Burgaleta, S. Arias, D. Ramirez, GEMASOLAR: the first tower thermo-solar commercial plant with molten salt storage, Proceed. SolarPACES (2011).

14. C.A. Amadei, G. Allesina, P. Tartarini, W. Yuting, Simulation of GEMASOLAR-based solar tower plants for the Chinese energy market: influence of plant downsizing and location change, Renewable Energy 55 (2013) 366–373.

15. Duffie JA, Beckman WA. Solar engineering of thermal processes. New York: Wiley; 1991.

16. W. B. Stine, R. W. Harrigon, Solar Energy Fundamentals and Design with Computer Application. New York: Wiley; 1985

17. K.K. Chong, M.H. Tan, Range of motion study for two different sun-tracking methods in the application of heliostat field; Solar Energy 85 (2011) 1837–1850.